npg

# The PET Radioligand [11C]MePPEP Binds Reversibly and with High Specific Signal to Cannabinoid CB1 Receptors in Nonhuman Primate Brain

**Fumihiko Yasuno[1], Amira K Brown[1], Sami S Zoghbi[1], Joseph H Krushinski[2], Eyassu Chernet[2], Johannes Tauscher[2], John M Schaus[2], Lee A Phebus[2], Amy K Chesterfield[2], Christian C Felder[2], Robert L Gladding[1], Jinsoo Hong[1], Christer Halldin[3], Victor W Pike[1] and Robert B Innis*[1]**

[1]*Molecular Imaging Branch, National Institute of Mental Health, Bethesda, MD, USA;* [2]*Lilly Research Laboratories, Lilly Corporate Center, Indianapolis, IN, USA and* [3]*Department of Clinical Neuroscience, Psychiatry Section, Karolinska Institutet, Stockholm, Sweden*

The cannabinoid CB1 receptor is one of the most abundant G protein-coupled receptors in the brain and is a promising target of therapeutic drug development. Success of drug development for neuropsychiatric indications is significantly enhanced with the ability to directly measure spatial and temporal binding of compounds to receptors in central compartments. We assessed the utility of a new positron emission tomography (PET) radioligand to image CB1 receptors in monkey brain. [11C]MePPEP ((3R,5R)-5-(3-methoxy-phenyl)-3-((R)-1-phenyl-ethylamino)-1-(4-trifluoromethyl-phenyl)-pyrrolidin-2-one) has high CB1 affinity ($K_b = 0.574 \pm 0.207$ nM) but also moderately high lipophilicity (measured $LogD_{7.4} = 4.8$). After intravenous injection of [11C]MePPEP, brain activity reached high levels of almost 600% standardized uptake value (SUV) within 10–20 min. The regional uptake was consistent with the distribution of CB1 receptors, with high radioactivity in striatum and cerebellum and low in thalamus and pons. Injection of pharmacological doses of CB1-selective agents confirmed that the tracer doses of [11C]MePPEP reversibly labeled CB1 receptors. Preblockade or displacement with two CB1 selective agents (ISPB; (4-(3-cyclopentyl-indole-1-sulfonyl)-N-(tetrahydro-pyran-4-ylmethyl)-benzamide) and rimonabant) showed that the majority (>89%) of brain uptake in regions with high receptor densities was specific and reversibly bound to CB1 receptors in the high binding regions. [11C]MePPEP was rapidly removed from arterial plasma. Regional brain uptake could be quantified as distribution volume relative to the concentration of parent radiotracer in plasma. The P-glycoprotein (P-gp) inhibitor DCPQ ((R)-4-[(1a,6,10b)-1,1-dichloro-1,1a,6,10b-tetrahydrodibenzo[a,e]cyclopropa[c]cyclohepten-6-yl]-[(5-quinolinyloxy)methyl]-1-piperazineethanol) did not significantly increase brain uptake of [11C]MePPEP, suggesting it is not a substrate for this efflux transporter at the blood–brain barrier. [11C]MePPEP is a radioligand with high brain uptake, high specific signal to CB1 receptors, and adequately fast washout from brain that allows quantification with 11C (half-life = 20 min). These promising results in monkey justify studying this radioligand in human subjects.

*Neuropsychopharmacology* (2007) **0**, 000–000. doi:10.1038/sj.npp.1301402

**Keywords:** cannabinoid; CB1 receptors; [11C]MePPEP; kinetic analysis; PET

## INTRODUCTION

Of the first two described cannabinoid receptor subtypes, the CB1 receptor is found mainly in the central nervous system, and the CB2 receptor is found mainly in peripheral immune system cells (Howlett *et al*, 2002). CB1 receptors are especially abundant in cerebellum, substantia nigra, globus pallidus, hippocampus, and lateral striatum (Herkenham

*et al*, 1990). The CB1 receptor mediates several pharmacological effects and is an active target for therapeutic drug development (Howlett *et al*, 2002; Le Foll and Goldberg, 2005). Cannabinoid receptor ligands may be useful for the treatment of pain (Walker *et al*, 1999), nausea (Simoneau *et al*, 2001), appetite control (Gelfand and Cannon, 2006; Kirkham and Tucci, 2006), and smoking cessation (Gelfand and Cannon, 2006).

The development of an *in vivo* imaging probe for the CB1 receptor has been difficult and largely unsuccessful. Similar to the active principal ingredient in marijuana, $\Delta^9$-tetrahydrocannabinol, most of the proposed radioligands are highly lipophilic. This physiochemical property commonly causes two deficiencies of radioligands. First, plasma protein binding tends to be high (>99%) so that only a

*Correspondence: Dr RB Innis, Molecular Imaging Branch, National Institute of Mental Health, Building 31, Room B2B37, 31 Center Drive, Bethesda, MD 20892-2035, USA, Tel: + 1 301 594 1368, Fax: + 1 301 480 3610, E-mail: robert.innis@nih.gov

2

small proportion ($<1\%$) is available to cross the blood–brain barrier. Second, brain has a high percentage of lipids, which comprise $\sim 60\%$ of its dry weight (Bennett and Horrobin, 2000). Thus, the majority of a lipophilic tracer that is able to cross the blood–brain barrier is often bound nonspecifically in the brain's abundant lipid environment. Thus, tracers that are too lipophilic tend to have low brain uptake and low ratios of specific to nonspecific binding. These two deficiencies apply to most radiotracers developed to date for the CB$_1$ receptor. These ligands have been based on the structures of rimonabant (Cosenza et al, 2000; Gatley et al, 1996; Horti et al, 2006; Katoch-Rouse et al, 2003; Mathews et al, 2000, 2002), cannabinoids (Charalambous et al, 1991), and alkylindoles (Gifford et al, 2002; Tamagan et al, 1999). In contrast to these older agents, $^{11}$C-JHU75528 is a notable exception (see 'Discussion') and has moderate brain uptake and specific signal (Horti et al, 2006).

To correct the deficiencies of most previous CB$_1$ receptor ligands, we recently developed [$^{11}$C]MePPEP (($3R,5R$)-5-(3-methoxy-phenyl)-3-(($R$)-1-phenyl-ethylamino)-1-(4-trifluoromethyl-phenyl)-pyrrolidin-2-one), which is a CB$_1$ mixed inverse agonist and antagonist (Figure 1). It has moderately high lipophilicity (measured Log$D_{7.4} = 4.8$) but still maintains high affinity and selectivity for the CB$_1$ receptor ($K_b$ at human CB$_1 = 0.574 \pm 0.207$ nM compared to CB$_2 = 363 \pm 87.4$ nM; see 'Results'). The primary purposes of this study were to carefully examine the kinetics of [$^{11}$C]MePPEP uptake in nonhuman primate brain and to determine whether human studies would be justified. Specifically, we assessed the pharmacological specificity of brain uptake and quantified the imaging data with compartmental modeling and serial arterial measurements of parent radiotracer separated from radiometabolites.

## MATERIALS AND METHODS

### [$\gamma$-$^{35}$S]GTP Binding Assay Methods

[$\gamma$-$^{35}$S]GTP binding was determined in a 96-well-plate format using a modification of the antibody capture scintillation proximity technique previously described (DeLapp et al, 1999). Briefly, 100 μl (0.9 units/well) of membrane preparation from Sf9 cells that ectopically express human CB$_1$ or CB$_2$ cannabinoid receptors (PerkinElmer Life and Analytical Sciences, Boston, MA) were incubated for 15 min with 50 μl of test compound diluted in 0.5% fatty acid-free bovine serum albumin (BSA) (Serologicals Corp., Norcross, GA). GDP was added to CB$_1$ (1 μM final concentration) and CB$_2$ (0.05 μM final concentration) receptor membranes before incubation. Antagonist/inverse agonist curves were generated in the presence of an EC$_{80}$ concentration of methanandamide and 0.5% BSA. Following the incubation period, 50 μl [$\gamma$-$^{35}$S]GTP (500 pM final concentration; PerkinElmer Life and Analytical Sciences, Boston, MA) were added to each well and incubated for 35 min. The labeled membranes were solubilized with 0.27% Nonidet P40 for 30 min followed by 30 min of incubation with 20 μl (final dilution of 1:300) of rabbit polyclonal G$\alpha_{i-3}$ antibody (Covance, Princeton, NJ). Following the antibody incubation, 50 μl (1.25 mg/well) anti-rabbit scintillation proximity assay beads (GE Healthcare, Piscataway, NJ) were added per well and the plates incubated for an
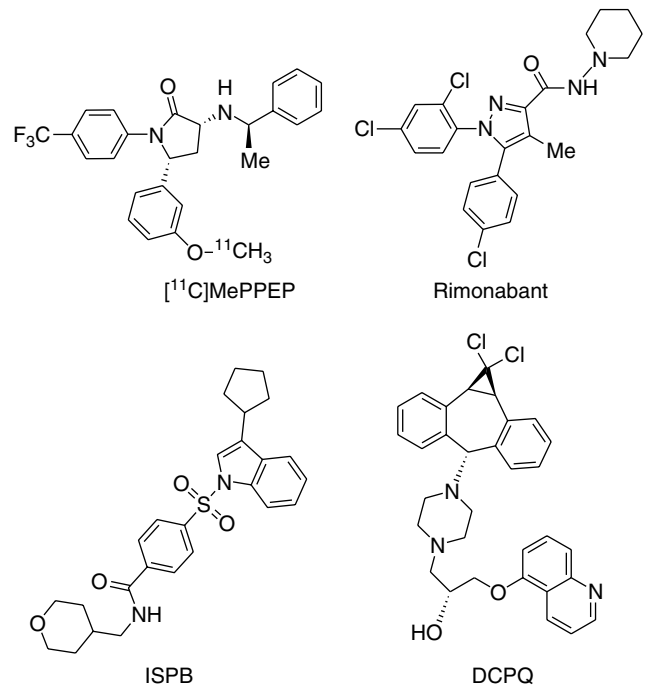


**Figure 1** Structures of [$^{11}$C]MePPEP, rimonabant, ISPB, and DCPQ.

additional 60 min. The plates were centrifuged for 10 min at 183$g$ and counted for 1 min per well using a Wallac MicroBeta TriLux scintillation counter (PerkinElmer, Boston, MA). All incubations took place at room temperature in GTP-binding assay buffer (20 mM HEPES, 100 mM NaCl, 5 mM MgC1$_2$, pH 7.4).

Data were analyzed using a four-parameter logistic-reduced fit with Marquardt–Levenberg algorithm and 200 iterations using Activity Base and XLFit2 (IDBS, Emeryville, CA). Background was subtracted from all wells, data were normalized to a full agonist response (1 μM methanandamide), and efficacy was expressed as a percentage of 1 μM methanandamide. Antagonist/inverse agonist percent inhibition data were normalized to results generated with an EC$_{80}$ concentration of methanandamide. $K_b$ values were determined using a modification of the Cheng–Prusoff relationship: $K_b = IC_{50}/(1 + (agonist)/EC_{50})$ where IC$_{50}$ is determined from a four parameter fit of displacement curves, [agonist] = EC$_{80}$ of full agonist (methanandamide), and EC$_{50}$ is determined from a four-parameter fit of the full agonist concentration response curve (Cheng and Prusoff, 1973). Mean EC$_{50}$ and percent inhibition values were calculated as a mean of three independent determinations $\pm$ standard error of the mean (SEM).

Broad screening of common cell surface targets was performed by standard radioligand binding techniques through a contract agreement with Cerep (Paris, France). Competitive binding was either not significant or had a $K_i$ value of $>10$ μM at the following receptor, ion channel, or enzyme targets: acetylcholinesterase, CCK1, CCK2, EDG-2, Cox1, Cox2, adenosine A1, adenosine A3, adrenergic alpha1, adrenergic alpha2, angiotensin AT1, adrenergic $\beta$1, adrenergic $\beta$2, benzodiazepine site, Ca$^{2+}$ channel (verapamil site), dopamine D1, dopamine D2S, GABA, Ghrelin, histamine H1, histamine H2, K$^+$ channel (HERG), non-

selective muscarinic, NE transporter, NK1, NK2, nonselective opiate, nonselective 5-HT.

## Preparation and Analysis of [¹¹C]MePPEP

[¹¹C]iodomethane produced by the GE PETtrace Microlab was delivered with helium carrier gas at a flow rate of 10 ml/min into a 2 ml stainless loop containing 1 mg phenolic precursor (22 nM) and 1 equivalent tetrabutylammonium hydroxide in 80 μl dimethyl formamide. The reaction proceeded for 5 min, and the entire contents of the loop were injected onto the HPLC column. The labeled product was purified on $C_{18}$ column (Phenomenex luna, $10 \times 250$ mm) with isocratic mobile phase ($70:30$ = acetonitrile/0.1 M ammonium formate, pH adjusted to 7.5 with 1 M ammonium hydroxide in water) at the flow rate of 6 ml/min. Product eluted at 12 min and precursor at 6.3 min. Solvents were removed by rotary evaporation at 80°C. The product was formulated with 10 ml saline containing 20 mg Tween 80 within 35 min of the end of bombardment.

## Measurement of Log$D_{7.4}$

[¹¹C]MePPEP was dissolved in 0.9% NaCl/10% ethanol to a specific concentration of about 10 μCi/μl. The radiochemical purity of this preparation was greater than 99%. Six determinations of Log$D_{7.4}$ were carried out at room temperature in n-octanol and 0.15 M phosphate buffer (pH 7.4), as previously described (Zoghbi *et al*, 1993), but with correction of the radioactivity associated with parent radioligand in the aqueous phase after radio-HPLC. The percent error of the γ-countermeasurements of the samples with the least counts was $4.6 \pm 0.3\%$.

## Animals

All animal experiments complied with the Guide for Care and Use of Laboratory Animals and were approved by the NIMH Animal Care and Use Committee. We used six male rhesus monkeys (weight: $12.6 \pm 2.0$ kg, with these and subsequent data expressed as mean $\pm$ SD), four of which underwent arterial blood sampling. Animals were immobilized with ketamine (10 mg/kg i.m.) for intubation. After transportation to the positron emission tomography (PET) suite, the animals were placed under isoflurane anesthesia (1–2%), and the head was immobilized in a stereotactic frame. To minimize the effects of ketamine, scans started at least 90 min after ketamine administration.

We used the high resolution research tomograph (HRRT; Siemens/CPS, Knoxville, TN, USA), which has a reconstructed resolution of 2.5 mm at full-width half-maximum in all directions in 3D mode. A transmission scan was initially performed for attenuation correction. [¹¹C]MePPEP was administered over ∼60 s. Scans of 120 min (33 frames) were acquired in all studies, whereas longer scans (39 frames over 150 min) were acquired in one monkey to evaluate the effect of the scan duration on the plasma compartmental analysis.

Arterial blood was collected in heparin-treated syringes from four monkeys at 15, 30, 45, 60, 75, 90, 105 s and 2, 3, 5, 10, 30, 60, 75, 90, 120 min after injection. The parent tracer, separated from radiometabolites, was measured as previously described (Zoghbi *et al*, 2005). We also measured the plasma-free fraction ($f_1$) of [¹¹C]MePPEP in two monkeys (E and F; Table 1). Plasma-free fraction was measured by ultrafiltration through Centrifree membrane filters (Amicon Division, W.R. Grace and Co., Danvers, MA, USA) (Gandelman *et al*, 1994) in two monkeys. Adequate radioactivity was used so that the percentage of counting error in the least radioactive samples ranged between $3.0 \pm 0.3$ and $5.3 \pm 1.3\%$ at one standard deviation.

Receptor preblocking studies were performed in two monkeys using rimonabant (previously called SR141716A) and ISPB (4-(3-cyclopentyl-indole-1-sulfonyl)-*N*-(tetrahydro-pyran-4-ylmethyl)-benzamide) (Figure 1), both of which are selective for the CB₁ receptor and have mixed inverse agonist and antagonist properties. ISPB (1.0 mg/kg i.v.) or rimonabant (3.0 mg/kg i.v.) were injected 10 min before [¹¹C]MePPEP (Table 1, monkeys A and B). A displacement study was also carried out for one monkey, in which nonradioactive ISPB (1.5 mg/kg i.v.) was injected 60 min after [¹¹C]MePPEP (Table 1, monkey A).

In this displacement study, data of the initial 9 min were not acquired because of a scanner problem. These studies of preblocking were performed in the afternoon, following the baseline scan of the same animal in the morning.

Each monkey had a T1-weighted magnetic resonance imaging (MRI) scan on a GE Sigma 1.5 T scanner (SPGR, TR/TE/flip angle = 13.1/5.8 ms/45°, $0.4 \times 0.4 \times 1.5$ mm with coronal acquisitions on a $256 \times 256 \times 60$ matrix).

## Image Analysis

Regional brain radioactivity was obtained with a modified template-based method that consisted of three steps (Yasuno *et al*, 2002). The first step involved the spatial transformation of the regional template from a model MRI

**Table 1** PET Studies Performed with [¹¹C]MePPEP

| Monkey | Arterial blood sampling | Plasma-free fraction | Scan duration (min) | Condition |
|---|---|---|---|---|
| A | + | − | 150/120[a] | Baseline and preblockade and displacement with ISPB |
| B | + | − | 120 | Baseline and preblockade with rimonabant |
| C | + | − | 120 | Baseline |
| D | + | − | 120 | Baseline and pretreatment with DCPQ (8.0 mg/kg) |
| E | − | + | 120 | Baseline and pretreatment with DCPQ (8.0 mg/kg) |
| F | − | + | 120 | Baseline and pretreatment with DCPQ (8.0 mg/kg) |

[a]150 min duration for the baseline and 120 min for preblockade.

4

to an individual animal's MRI. The second step was the manual correction of the error of transformed volumes of interest with reference to the animal's MRI (Figure 2). Finally, corrected template volumes were linearly transformed to the PET images using the parameters obtained from the coregistration of the MRI. Seven template volumes were defined: cerebellum (2.1 cm$^3$), prefrontal cortex (8.8 cm$^3$), lateral temporal cortex (5.9 cm$^3$), medial temporal region including the hippocampus (3.1 cm$^3$), striatum (2.7 cm$^3$), thalamus (0.9 cm$^3$), and pons (0.8 cm$^3$).

### Estimation of Distribution Volume with Arterial Input Function

The brain and plasma data were analyzed with one- and two-tissue compartment models using rate constants ($K_1$, $k_2$, $k_3$, and $k_4$) as previously described (Laruelle et al, 1994). Total distribution volume $V_T$ measures specific receptor binding, nonspecific binding, and free radiotracer. The nondisplaceable component $V_{ND}$ is the sum of the latter two—nonspecific binding plus free radiotracer.

For the one-tissue compartment model:

$$V_T = \frac{K_1}{k_2}$$

For the two-compartment model, $V_T$ is the sum of the distribution volumes of nondisplaceable uptake ($V_{ND}$) and specific binding ($V_S$).

$$V_{ND} = \frac{K_1}{k_2}$$
$$V_S = \frac{K_1 k_3}{k_2 k_4}$$
$$V_T = V_{ND} + V_S$$
$$= \left(\frac{K_1}{k_2}\right)\left(1 + \frac{k_3}{k_4}\right)$$

The kinetic analyses were performed using the software program PMOD 2.75 (Burger et al, 1998).
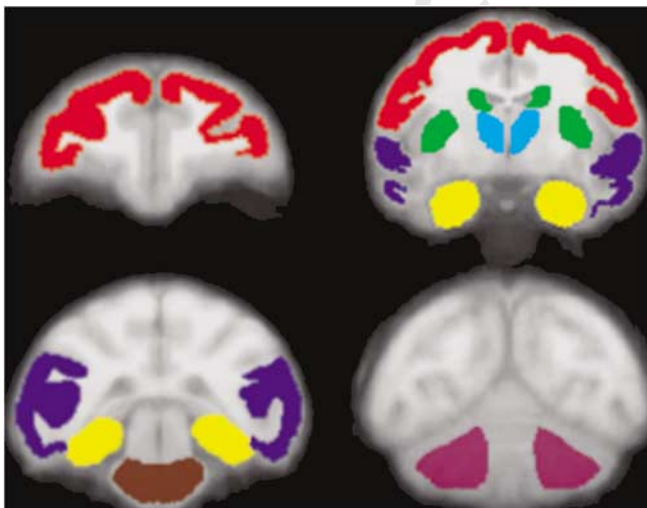


**Figure 2** Volume of interest template defined on the model MRI. Red, prefrontal cortex; dark blue, lateral temporal cortex; yellow, medial temporal region (including hipppocampus); green, striatum; light blue, thalamus; brown, pons; purple, cerebellum.

### Time-Stability of Parameter Estimates

The relationship between parameter estimates and the duration of the scan was analyzed in one monkey with increasingly truncated data sets from 0–150 to 0–60 min (Table 1, monkey A). The estimated parameters were compared with the reference values obtained with the complete 150 min data set. For the time activity data from the mean of all measured regions, specific binding was estimated in the two-tissue compartmental model. The solution was considered stable after time $t$ if the result was within 10% of that from the analysis of the entire data set (ie 0–150 min).

### Effect of P-gp on Brain Uptake and Peripheral Disposition of [$^{11}$C]MePPEP

We compared the uptake of [$^{11}$C]MePPEP in three studies (Table 1, monkey D, E, and F) with and without the administration of 8 mg/kg i.v. of the P-glycoprotein (P-gp) inhibitor DCPQ (($R$)-4-[(1a,6,10b)-1,1-dichloro-1,1a,6,10b-tetrahydrodibenzo[a,e]cyclopropa[c]cyclohepten-6-yl]-[(5-quinolinyloxy)methyl]-1-piperazineethanol; Figure 1). DCPQ was previously reported as compound 14b (Pfister et al, 1995).

Under terms of the Material Transfer Agreement with Xenova Group, Ltd (UK) we could not use their better known P-gp inhibitor tariquidar, previously called XR9576 (Roe et al, 1999) with proprietary compounds in the current collaboration. Instead, we compared the efficacy of tariquidar and DCPQ to enhance brain uptake of [$^{11}$C]lo-pramide, which is an avid substrate for P-gp (Sadeque et al, 2000). DCPQ and tariquidar (each at 8 mg/kg i.v.) was administered 30 min before [$^{11}$C]loperamide and increased rhesus brain activity to 415 and 316%, respectively.

### Statistical Analysis

Goodness-of-fit by nonlinear least-squares analysis was evaluated using the model selection criterion (MSC), which is a modification of the Akaike information criterion (Akaike, 1974). MSC gives greater values for better fitting. Goodness-of-fit by one- and two-tissue compartmental models was compared with F statistics (Hawkins et al, 1986).

The standard error of nonlinear least-squares estimation for rate constants was given by the diagonal of the covariance matrix (Carson, 1986) and expressed as a percentage of the rate constants (coefficient of variation, %COV). In addition, %COV of total distribution volume was calculated from the covariance matrix using the generalized form of error propagation equation (Bevington and Robinson, 2003), where correlations among parameters were taken into account.

### RESULTS

### In Vitro Activity of MePPEP

In membranes prepared from Sf9 cells ectopically expressing the human CB$_1$ or CB$_2$ receptors, in vitro functional binding activity of nonlabeled MePPEP was determined

using an antibody capture scintillation proximity [$\gamma$-$^{35}$S]GTP binding assay and compared to rimonabant (previously called SR141716A). MePPEP inhibited functional [$\gamma$-$^{35}$S]GTP binding at the human CB$_1$ receptor with high potency ($K_b = 0.574 \pm 0.207$ nM) compared to rimonabant ($K_b = 5.96 \pm 0.209$ nM). MePPEP was significantly less potent at the human CB$_2$ receptor ($K_b = 363 \pm 77.9$ nM for MePPEP and $K_b > 10\,000$ nM for rimonabant at CB$_2$).

## Preparation of [$^{11}$C]MePPEP

The radioligand was prepared within 35 min of the end of bombardment and had yield $= 2.5 \pm 1.1\%$, radiochemical purity $= 100 \pm 0\%$, chemical purity $= 99.9 \pm 0\%$, and specific activity at time of injection $= 78.1 \pm 54.9$ GBq/$\mu$M ($n = 12$ batches). The mean injected activity was $232 \pm 70$ MBq.

The Log$D_{7.4}$ of [$^{11}$C]MePPEP was $4.8 \pm 0.3$ ($n = 6$), measured in octanol/saline at pH 7.4.

## Pharmacological Effects in Nonhuman Primates

In PET scans, the injected mass dose of [$^{11}$C]MePPEP was $0.11 \pm 0.06$ $\mu$g/kg. In all baseline and blocking experiments using ISPB (1.0–1.5 mg/kg) and rimonabant (3.0 mg/kg), the differences between pre- and postinjection vital signs were: $<17$ mm Hg for systemic blood pressure, $<17$ min$^{-1}$ for pulse, $<3$ min$^{-1}$ for respiratory rate, and $<0.1^\circ$C for temperature.

## Brain Uptake of [$^{11}$C]MePPEP

Following injection of [$^{11}$C]MePPEP, brain activity increased to high levels (almost 600% standardized uptake (SUV) in cerebellum), with peak values within 10–20 min. The distribution of activity was consistent with binding to CB$_1$ receptors, with high levels in striatum and cerebellum and low in thalamus and pons (Figures 3 and 4a). The brain uptake of [$^{11}$C]MePPEP was preblocked with receptor saturating doses of nonradioactive ISPB (1.0 mg/kg i.v.) or rimonabant (3.0 mg/kg i.v.) (Figure 4b). In addition, brain uptake was rapidly displaced by nonradioactive ISPB (1.5 mg/kg i.v.) at 60 min after tracer injection (Figure 4c). In summary, brain uptake of [$^{11}$C]MePPEP was consistent with reversible labeling of CB$_1$ receptors, showing an appropriate regional distribution, pharmacological selectivity, and saturability.

## Arterial Plasma Analysis

The radioligand was quickly metabolized and represented $83 \pm 12$, $53 \pm 17$, $21 \pm 7$, and $14 \pm 5\%$ of total plasma activity at 5, 10, 30, and 60 min, respectively, in all the four monkey studies. [$^{11}$C]MePPEP was rapidly removed from arterial plasma, with a clearance rate of $361 \pm 40$ ml/min. Plasma activity of unchanged [$^{11}$C]MePPEP peaked at $\sim 1$ min and decreased to $3.1 \pm 0.9\%$ of the peak by 10 min.

Monkey arterial plasma samples had four radioactive peaks. A sample radiochromatogram of plasma at 10 min (Figure 5a) was composed of polar peak 1 (34.4%); two intermediate peaks, 2 (5.4%) and 3 (1.2%); and parent radioligand 4 (59%). The plasma parent composition declined rapidly to about 18% as early as 30 min after the

injection of [$^{11}$C]MePPEP. Radiometabolite 1 was the major radioactive component at the end of the study (Figure 5b).

## Nonlinear Least-Squares Compartmental Analyses

We used brain activity and serial arterial plasma measurements of parent radiotracer to estimate distribution volume in brain using four scanning sessions in four different animals (monkeys A–D; Table 1). Convergence was achieved in the baseline scans using both one- and two-tissue compartmental model analyses of 120 min scan data, but the two-tissue compartmental model provided significantly better fits (Tables 2 and 3; Figure 6). MSC values were higher for two-tissue ($3.4 \pm 0.7$) than for one-tissue ($2.2 \pm 0.7$) compartmental models, and this difference was significant by $F$-test in all regions of all animals ($p < 0.001$).

In two-tissue compartmental model, the standard errors of individual rate constants showed poor identifiability with COV values $>10\%$ in most regions. However, $V_S$ and $V_T$ were relatively well identified in each model, with COV values $<8\%$. Although values of $V_T$ obtained with the one- and two-tissue compartment models correlated well ($r = 0.99$), the one-tissue model apparently underestimated $V_T$ by an average of 12% (range 426%), which may have been caused by its relatively poor goodness of fit.

We also calculated distribution volume in two scanning sessions (monkeys A and B, Table 1) with preblockade of rimonabant or ISPB and compared them to the baseline $V_T$ of same animals. In these two studies, the mean regional value of nondisplaceable uptake ($V_{ND}$) in high binding regions (ie all except thalamus and pons) was about 11% of $V_T$ (Table 4). Thus, we estimate that 89% of total brain uptake was associated with CB$_1$ receptors.

## Effect of P-gp on Brain Uptake and Peripheral Disposition of [$^{11}$C]MePPEP

DCPQ (8 mg/kg i.v.) significantly increased the uptake of [$^{11}$C]MePPEP in all brain regions (Figure 7a). In contrast, DCPQ had no significant effect on the clearance of [$^{11}$C]MePPEP measured in arterial plasma corrected for radiometabolites (Figure 7b). In the three animals tested, DCPQ caused a $\sim 17\%$ increase of the mean area under the brain curves of all six regions, calculated from 0 to 120 min (Table 5). These results showed an apparent effect of P-gp blockade—increased brain uptake in the absence of noticeable changes of total tracer concentration in plasma. However, we also examined the effect of DCPQ on $f_1$ of tracer. DCPQ increased $f_1$ in each animal, with a mean increase of 10% (Table 5).

Correction of the area under the curve for change in $f_1$ suggested that DCPQ caused only a 6% effect on brain activity independent of its peripheral effects. That is, the corrected ratio under the brain activity curves between baseline and DCPQ was 1.06 ($= 1.17/1.10$). An increase of 6% with P-gp blockade is quite small relative to tracers that are known to be efflux pump substrates, which are elevated 400–1300% with genetic inactivation of P-gp (Schinkel et al, 1996). This 6% increase may also be insignificant in light of possible measurement errors for the small absolute values of $f_1$ (0.04–0.07%; Table 5).
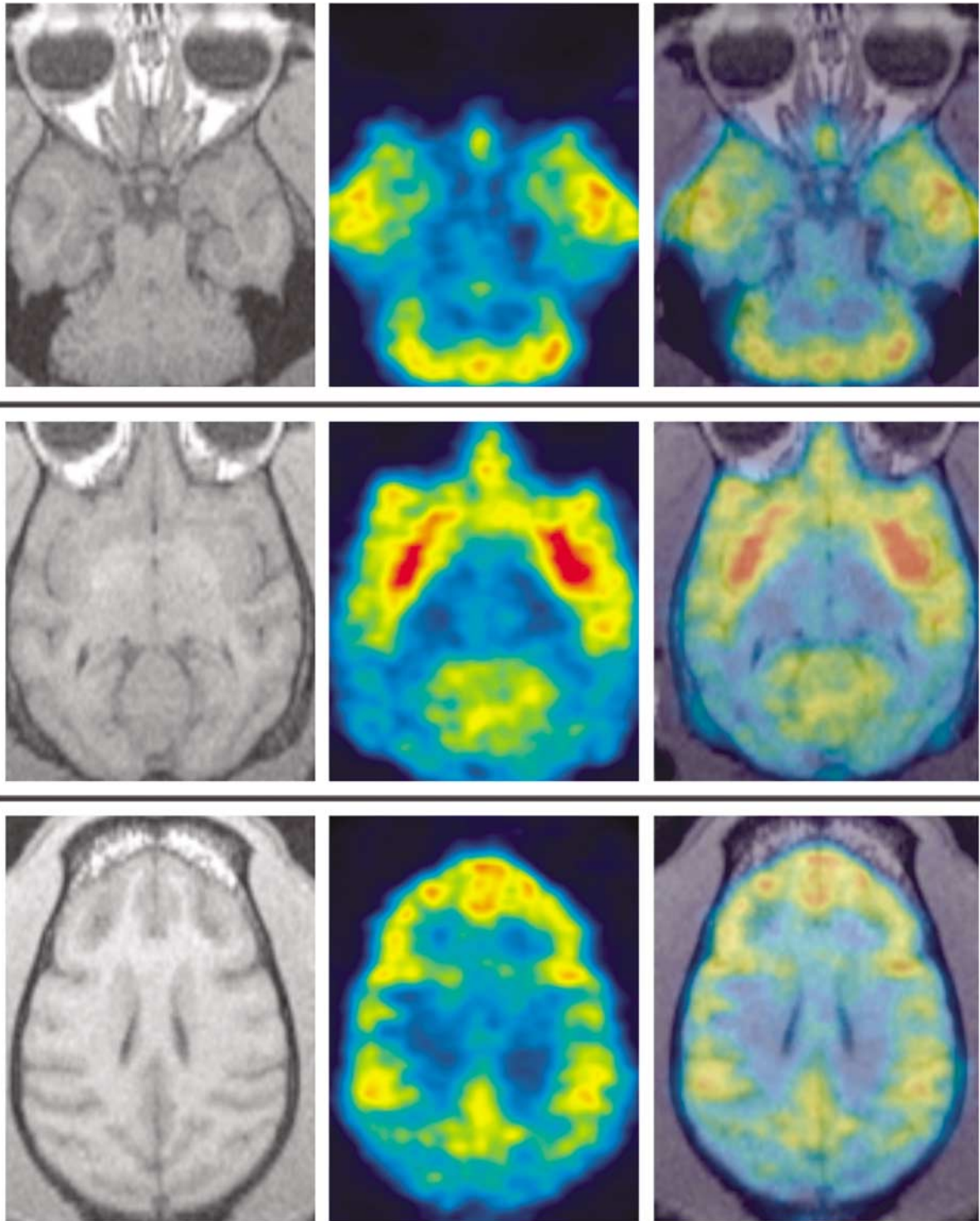
**Figure 3** PET summation image in rhesus brain. PET images (middle column) were summed from 60 to 120 min. The corresponding MR images are on left column, and the fused PET and MR images are on right column. Upper row: slice including cerebellum and medial and lateral temporal cortex. Middle row: slice including striatum, thalamus, and lateral temporal cortex. Lower row: slice including prefrontal cortex.

## DISCUSSION

The uptake of [$^{11}$C]MePPEP in nonhuman primate brain demonstrated reversible labeling of CB$_1$ receptors. Brain uptake showed appropriate pharmacological properties, as it could be displaced and/or blocked by agents from two different chemical classes, ISPB and rimonabant. The clearance of [$^{11}$C]MePPEP in monkey was adequately fast to generate peak brain uptake within 20 min, which is well within the effective imaging time of $^{11}$C that has a half-life of 20 min.

The P-gp inhibitor DCPQ (8 mg/kg i.v.) increased brain uptake by $\sim$17%, with insignificant change in the parent tracer in plasma (ie the amount of tracer exposed to brain;
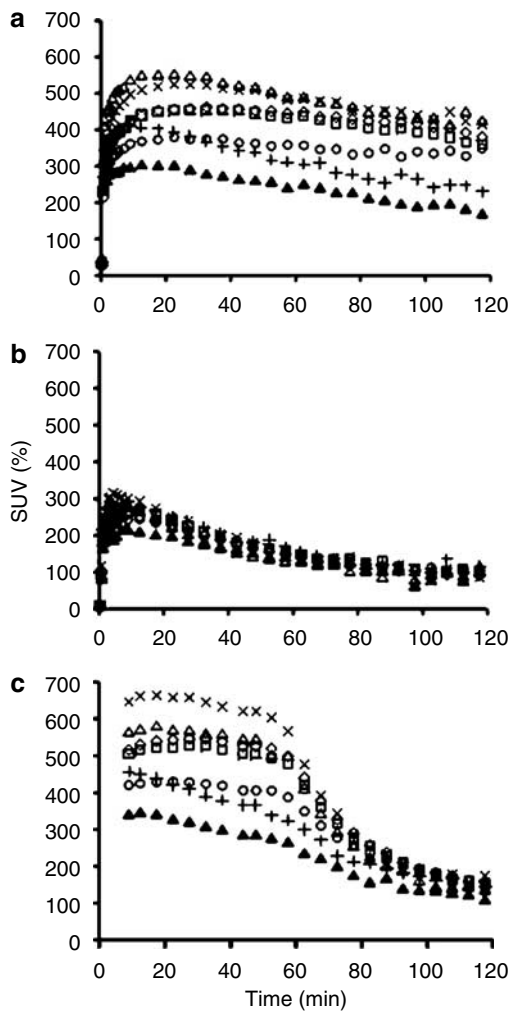
**Figure 4** (a) Time course of regional brain activities after injection of [$^{11}$C]MePPEP. Activity is shown as %SUV which normalizes for injected dose and body weight. %SUV = (% injected activity/cm$^3$ tissue)(g body weight) cerebellum, $\triangle$; striatum, $\times$; prefrontal cortex, $\diamond$; lateral temporal cortex, $\square$; medial temporal region, $\bigcirc$; thalamus, +; and pons, ▲. (b) Receptors were blocked by pretreatment with ISPB (1.0 mg/kg i.v.) before injection of [$^{11}$C]MePPEP. (c) Radioligand was displaced by ISPB (1.5 mg/kg i.v.) injected 60 min after [$^{11}$C]MePPEP. Data from the initial 9 min are missing because of scanner malfunction.

**Q1** Figure 8). However, DCPQ increased $f_1$ by $\sim 10\%$, and the corrected ratio of area under the curve between baseline and DCPQ was 1.06 ( = 1.17/1.10), which may merely reflect errors in measurement of the low values of $f_1$ (Table 5). In addition, a 17% increase is small compared to >400% found for agents that are avid substrates for P-gp (Schinkel et al, 1996). Thus, our data suggest that [$^{11}$C]MePPEP is a relatively insignificant substrate for P-gp in monkey brain.

## Advantages of [$^{11}$C]MePPEP

What are the relative advantages and limitations of [$^{11}$C]MePPEP as a probe for central CB$_1$ receptors? The advantages include:
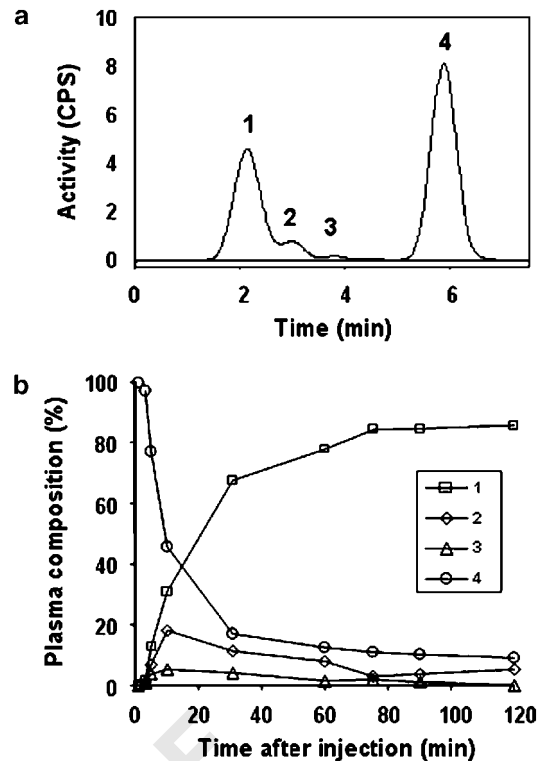


**Figure 5** (a) Radiochromatogram of a plasma sample obtained at 10 min after intravenous injection of [$^{11}$C]MePPEP. Peak 1 was the most polar radiometabolite and eluted in the void volume of the column. Peak 4 was the parent radioligand. (b) Representative plasma composition over time of [$^{11}$C]MePPEP (4) and its three radiometabolites (1, 2, and 3).

(1) [$^{11}$C]MePPEP has high brain uptake, with peak levels of almost 600% SUV. Such high uptake means that brain activity can be more accurately quantified and/or the injected activity can be reduced. For comparison, the peak uptake of two other PET radiotracers in monkey is 300% SUV in striatum for the dopamine D$_{2/3}$ receptor probe [$^{11}$C]raclopride (Nyberg et al, 2002) and 500% SUV in medial temporal region for the 5-HT$_{1A}$ receptor probe [$^{11}$C](R)-(−)-RWAY (Yasuno et al, 2006). The high brain uptake of [$^{11}$C]MePPEP reflected, in part, CB$_1$ receptor density, which is the highest of any G protein-coupled receptor in brain (Begg et al, 2005). The density ($B_{max}$) of CB$_1$ receptors in cerebellum in rat is 1752 fmol/mg protein (Hirst et al, 1996), compared to dopamine D$_2$ receptors in striatum ($B_{max} = 247$ fmol/mg protein) (Dewar et al, 1989) and 5-HT$_{1A}$ receptors in hippocampal region (312 fmol/mg protein) (Khawaja et al, 1995).

(2) [$^{11}$C]MePPEP has a high percentage of specific binding. We performed compartmental analysis in two different preblocked conditions. The results suggested at least 89% of uptake was specific in high binding regions. If we had administered a dose that completely blocked CB$_1$ receptors, then the estimate of specific uptake would have been even higher. In summary, both baseline and preblocked analysis showed that the vast majority (>89%) of brain uptake is bound to CB$_1$ receptors (ie specific binding).

**Table 2** Parameter Estimates (Mean±SD) Obtained from a Two-Tissue Compartment Model

| Region | $K_1$ (ml min$^{-1}$ cm$^{-3}$) %COV | $k_2$ (min$^{-1}$) %COV | $k_3$ (min$^{-1}$) %COV | $k_4$ (min$^{-1}$) %COV | $V_S$ (ml cm$^{-3}$) %COV | $V_T$ (ml cm$^{-3}$) %COV | MSC |
|---|---|---|---|---|---|---|---|
| Prefrontal cortex | 0.22±0.08 | 0.70±0.21 | 1.20±0.44 | 0.01±0.004 | 53.5±24.7 | 53.8±24.9 | 4.8±0.6 |
| | 6.3±5.4 | 22.6±18.4 | 7.5±6.0 | 13.6±9.6 | 5.2±4.2 | 5.2±4.2 | |
| Lateral temporal | 0.24±0.09 | 0.71±0.25 | 1.13±0.38 | 0.01±0.004 | 42.7±20.8 | 43.1±20.9 | 5.1±0.3 |
| Cortex | 4.9±2.6 | 14.7±10.0 | 7.1±3.3 | 8.8±4.2 | 2.8±1.2 | 2.7±1.2 | |
| Medial temporal | 0.23±0.11 | 0.62±0.15 | 0.67±0.07 | 0.01±0.003 | 36.4±15.8 | 36.8±15.9 | 3.8±1.3 |
| Region | 11.6±8.2 | 31.4±15.3 | 13.7±5.2 | 11.7±3.6 | 5.4±2.5 | 5.4±2.5 | |
| Striatum | 0.27±0.15 | 0.59±0.30 | 1.02±0.40 | 0.01±0.004 | 46.9±19.1 | 47.4±19.3 | 4.3±0.3 |
| | 8.0±2.3 | 45.1±34.2 | 25.0±20.6 | 15.9±15.0 | 4.8±4.1 | 4.8±4.2 | |
| Thalamus | 0.23±0.09 | 0.54±0.40 | 0.63±0.27 | 0.02±0.004 | 16.2±8.0 | 16.7±8.3 | 3.1±0.5 |
| | 8.4±3.2 | 34.8±25.3 | 21.3±15.3 | 12.1±7.0 | 3.1±1.0 | 2.8±0.6 | |
| Cerebellum | 0.29±0.11 | 0.54±0.52 | 0.68±0.53 | 0.01±0.002 | 32.2±12.5 | 33.4±12.5 | 3.5±0.6 |
| | 10.3±8.6 | 42.0±13.2 | 24.9±10.4 | 14.9±4.8 | 4.2±2.5 | 4.1±2.5 | |
| Pons | 0.28±0.11 | 1.86±1.14 | 0.97±0.21 | 0.01±0.003 | 16.2±7.4 | 16.4±7.5 | 3.1±0.9 |
| | 15.8±1.2 | 37.4±13.6 | 16.5±11.2 | 11.7±7.5 | 4.6±4.3 | 4.6±4.3 | |

COV, coefficient of variation; MSC, model selection criteria; SD, standard deviation; $V_S$, specific binding potential; $V_T$, total distribution volume.
The values on the first of two lines for each region are the mean±SD of the parameter determined in three scanning studies.
The values on the second line are the identifiability of the parameter (called 'standard error' of the compartmental fit) and are expressed as %COV. For example, $K_1$ in prefrontal cortex was 0.22±0.08 ml min$^{-1}$ cm$^{-3}$ and had a mean±SD identifiability of 6.3±5.4% of that value.

**Table 3** Parameter Estimates (Mean±SD) Obtained from a One-Tissue Compartment Model

| Region | $K_1$ (ml min$^{-1}$ cm$^{-3}$) %COV | $k_2$ (min$^{-1}$) %COV | $V_T$ (ml cm$^{-3}$) %COV | MSC |
|---|---|---|---|---|
| Prefrontal cortex | 0.14±0.04 | 0.003±0.001 | 46.0±18.8 | 3.5±0.3 |
| | 1.3±0.3 | 7.8±3.7 | 6.8±3.4 | |
| Lateral temporal cortex | 0.15±0.04 | 0.004±0.001 | 37.9±16.2 | 3.4±0.4 |
| | 1.3±0.3 | 6.1±2.2 | 5.1±2.0 | |
| Medial temporal region | 0.13±0.05 | 0.004±0.001 | 29.5±12.3 | 1.9±0.4 |
| | 2.3±0.01 | 10.0±1.9 | 8.3±1.9 | |
| Striatum | 0.18±0.07 | 0.004±0.002 | 42.1±15.7 | 3.1±0.4 |
| | 1.4±0.3 | 6.7±2.9 | 5.6±2.7 | |
| Thalamus | 0.1±0.05 | 0.010±0.002 | 15.2±7.0 | 1.9±0.2 |
| | 2.31±0.21 | 5.7±0.7 | 4.2±0.6 | |
| Cerebellum | 0.2±0.06 | 0.006±0.001 | 29.4±11.1 | 2.3±0.2 |
| | 1.9±0.2 | 6.0±1.0 | 4.7±0.8 | |
| Pons | 0.11±0.04 | 0.008±0.003 | 14.7±6.6 | 1.5±0.2 |
| | 2.7±0.3 | 8.3±2.7 | 6.4±1.9 | |

COV, coefficient of variation; MSC, model selection criteria; SD, standard deviation; $V_T$, total distribution volume.
See legend of Table 1 for meaning of values on upper and lower lines for each region.

(3) The rapid plasma clearance of [$^{11}$C]MePPEP is important to measure distribution volume. As a general rule, quantitation of brain uptake requires imaging before and slightly after the time of peak uptake. Receptor density and plasma clearance have opposite effects on the time of peak uptake. That is, higher densities of receptors cause later times of peak uptake, as these regions can bind more ligand at equilibrium. In contrast, faster plasma clearance causes an earlier peak in all organs, because the ligand is removed from the body more rapidly. As CB$_1$ receptors are present at such high densities in brain, the clearance of a useful radioligand must be rapid so that the peak can occur within the useful imaging time of the radionuclide. Thus, the rapid plasma clearance of [$^{11}$C]MePPEP (see 'Results') is critical to quantify distribution volume, which is proportional to receptor density.

NPG.NPP.1301402

(4) [¹¹C]MePPEP is relatively easily prepared with high purity (>99%) and in reasonable overall yield (3%) using a commercially available ¹¹C-methylation apparatus.

(5) The short half-life of ¹¹C allows two or more scanning studies to be completed in a single subject in 1 day. Such a repeated scanning schedule can accommodate pharmacological challenges or measurements of receptor occupancy by CB₁ receptor-selective medications.

## Limitation of [¹¹C]MePPEP

The limitations of [¹¹C]MePPEP and imaging the CB₁ receptor in general include:
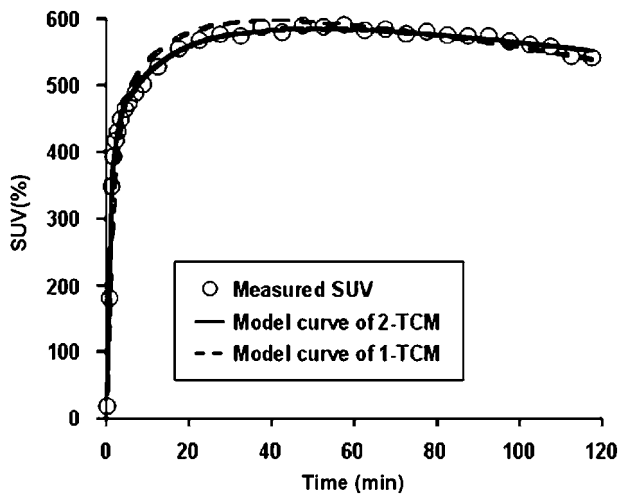
**Figure 6** One- and two-tissue compartment analysis. Fitting by two-tissue compartmental model (solid line) was significantly better that that by one-tissue compartmental model (dashed line) for measured %SUV of all regions. The %SUV of all regions was calculated from the volume-weighted average of cerebellum, striatum, prefrontal cortex, lateral temporal cortex, medial temporal region, and pons.

(1) The plasma-free fraction $f_1$ of [¹¹C]MePPEP was quite low (0.04–0.07%) and difficult to measure accurately. Brain uptake is proportional to $f_1$, as protein-bound drug cannot cross the blood–brain barrier. Thus, relatively small changes in protein binding would have significant effects on total brain uptake. For example, if protein binding decreases from 99.9 to 99.8%, then $f_1$ and brain uptake would increase 100%, from 0.1 to 0.2%. Intersubject variability of baseline distribution volumes in our studies may not reflect actual differences in receptor densities. Instead, it may reflect biological variability in $f_1$ or our limited accuracy to measure such low values. Future studies should carefully assess methods to accurately measure and assess the impact of $f_1$ on brain uptake of [¹¹C]MePPEP.

(2) Although not a limitation specific to [¹¹C]MePPEP, the monkey brain has no region that could be used as reference tissue. We quantified brain uptake relative to concentrations of parent radiotracer in plasma. Reference tissue methods compare uptake in receptor-rich to receptor-free regions within brain and are much simpler to perform. Even the pons, which has a relatively low density of CB₁ receptors, showed significant displacement and blockade (Figure 4b and c). Some of this displaceable activity derived from surrounding regions, because of the limited resolution of the PET camera and the resulting spillover of activity from adjacent tissue. The human brain may be large enough so that a small area like pons could be used as a reference region. Analysis with a reference region would not only avoid arterial plasma sampling but also obviate the need to measure $f_1$. That is, normalizing to a reference region effectively corrects for intersubject variations in $f_1$.

(3) [¹¹C]MePPEP may generate radiometabolite(s) that enter monkey brain. The vast majority of brain activity was displaced or preblocked, suggesting that any putative metabolite must retain significant receptor

**Table 4** Total Distribution Volume of Baseline and Preblocking Study of Two Monkeys

| Region | $V_T$ (baseline) | $V_T$ (preblocking study) | % of baseline/preblocking | Average of % |
|---|---|---|---|---|
| Prefrontal cortex | 26.0 | 2.8 | 10.9 | 9.3 |
| | 63.3 | 5.0 | 7.8 | |
| Lateral temporal cortex | 22.4 | 3.0 | 13.4 | 11.6 |
| | 54.7 | 5.3 | 9.8 | |
| Medial temporal region | 19.1 | 3.0 | 15.4 | 13.6 |
| | 43.1 | 5.0 | 11.7 | |
| Striatum | 24.3 | 2.9 | 12.1 | 10.8 |
| | 53.8 | 5.1 | 9.5 | |
| Thalamus | 10.8 | 3.1 | 28.2 | 25.6 |
| | 23.3 | 5.4 | 23.0 | |
| Cerebellum | 21.7 | 2.5 | 11.6 | 10.7 |
| | 42.2 | 4.2 | 9.9 | |
| Pons | 8.6 | 2.6 | 30.0 | 25.3 |
| | 21.6 | 4.4 | 20.5 | |

$V_T$, total distribution volume.
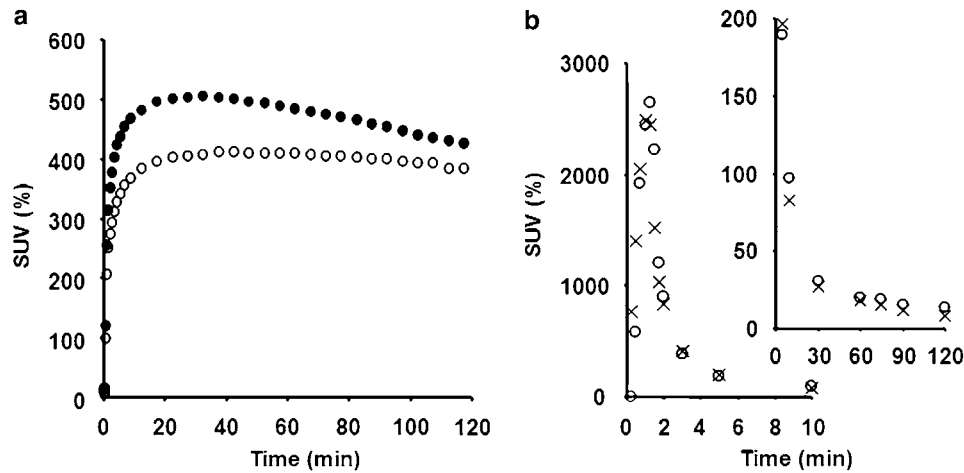Upper: Monkey A, preblockade with rimonabant; Lower: Monkey B, preblockade with ISPB.

**Figure 7** Effect of DCPQ on brain uptake and peripheral clearance of [$^{11}$C]MePPEP. (a) Average uptake of all measured regions of all animals. DCPQ (8 mg/kg i.v.) increased uptake in all regions. Open circles represent baseline and solid circles DCPQ results. (b) [$^{11}$C]MePPEP plasma radioactivity, corrected for metabolites, are shown for baseline (O) and P-gp inhibitor (×) studies. Values are total concentration of plasma [$^{11}$C]MePPEP—free plus protein bound. Left curve shows values from 0 to 10 min; right curve from 5 to 120 min. The curves suggest no significant effect of P-gp inhibition on peripheral clearance.

**Table 5** Brain AUC and Plasma-Free Fraction ($f_1$): Baseline and after DCPQ Administration

| Monkey | $f_1$ (%) | | Ratio: DCPQ/baseline | |
| | Baseline | DCPQ | $f_1$ | AUC |
| --- | --- | --- | --- | --- |
| D | — | — | — | 1.21 |
| E | 0.042 | 0.044 | 1.05 | 1.13 |
| F | 0.055 | 0.063 | 1.15 | 1.17 |
| Mean ± SD | 0.049 ± 0.009 | 0.054 ± 0.013 | 1.10 ± 0.07 | 1.17 ± 0.04 |

AUC, area under the curve.
Brain AUC was calculated for all six regions from 0 to 120 min.

affinity. Nevertheless, additional studies in rodents would be useful to detect the presence and the level of radiometabolites extracted from brain, and any future human studies with [$^{11}$C]MePPEP should carefully examine the time stability of distribution volume measurements.

(4) A major concern about [$^{11}$C]MePPEP is whether humans will have slower brain washout such that distribution volume measurements are unstable within the practicable imaging time of $^{11}$C. Scans typically span a total 60–150 min, depending on injected activity and sensitivity of the camera. Brain washout is highly dependent on the peripheral clearance of the radiopharmaceutical, with faster peripheral clearance causing fasting brain washout. In the absence of pharmacokinetic data on MePPEP, human studies with tracer doses of [$^{11}$C]MePPEP are the most expeditious method to determine the utility of the radiotracer. Because of its overall favorable performance in monkeys, we plan to study [$^{11}$C]MePPEP in humans.

## Comparison with Other CB$_1$ Receptor Radioligands

$^{11}$C-JHU75528 is an analog of rimonabant and was recently reported as an effective PET probe for CB$_1$ receptors (Horti et al, 2006). As mentioned in the 'Introduction', it appears to be the best radioligand published to date for in vivo imaging of the CB$_1$ receptor. $^{11}$C-JHU75528 and [$^{11}$C]MeP-PEP had similar distribution and time of peak uptake ($\sim$20 min) in baboon and rhesus brain, respectively. However, the peak uptake of $^{11}$C-JHU75528 may be almost sixfold lower than that of [$^{11}$C]MePPEP. The brain peak uptake of $^{11}$C-JHU75528 is reported to be 0.4% injected activity per 100 ml in putamen in male baboon (26 kg), which corresponds to an SUV of 104%. In contrast, [$^{11}$C]MePPEP showed peak striatal uptake of $\sim$600% SUV in our study. The percentage-specific binding of these two tracers is difficult to compare, because of different measurements in the two studies. Nevertheless, preblockade decreased striatal uptake of $^{11}$C-JHU75528 by about 50%, which is similar to our results with [$^{11}$C]MePPEP (Figure 4a and b). Note that these comparisons of brain time activity curves do not correct for changes in arterial input function, which are required for accurate quantitation of the percentage-specific signal in brain. In brief, [$^{11}$C]MePPEP and $^{11}$C-JHU75528 appear to have fairly similar kinetics of brain uptake and may have similar percentage of specific signal. However, the peak uptake of [$^{11}$C]MePPEP is about sixfold greater than that of $^{11}$C-JHU75528. Both $^{11}$C-JHU75528 and [$^{11}$C]MePPEP are likely to be assessed in humans. Because these two ligands have different structures, species differences in clearance, metabolism, and plasma protein binding may make one tracer clearly superior to the other for human studies.

## Conclusion

[$^{11}$C]MePPEP is promising tracer to measure CB$_1$ receptors. It readily entered monkey brain, had peak levels within 20 min, and showed relatively stable measurements of

distribution volume within 90 min. For quantitation of distribution volumes using an arterial input, the two-tissue compartment analysis was superior to one-tissue for all measured regions. These promising results justify trials of [$^{11}$C]MePPEP in humans, for which brain uptake should be carefully analyzed for measuring distribution volume parameters and to provide any evidence of radiometabolites.

## REFERENCES

Akaike H (1974). A new look at the statistical model identification. *IEEE Trans Automat Control AC* **19**: 716–723.

Begg M, Pacher P, Batkai S, Osei-Hyiaman D, Offertaler L, Mo FM *et al* (2005). Evidence for novel cannabinoid receptors. *Pharmacol Ther* **106**: 133–145.

Bennett CN, Horrobin DF (2000). Gene targets related to phospholipid and fatty acid metabolism in schizophrenia and other psychiatric disorders: an update. *Prostaglandins Leukot Essent Fatty Acids* **63**: 47–59.

Bevington PR, Robinson DK (2003). *Data Reduction and Error Analysis for the Physical Sciences*. McGraw-Hill: New York.

Burger C, Mikolajczyk K, Grodzki M, Rudnicki P, Szabatin M, Buck A (1998). JAVA tools quantitative post-processing of brain PET data. *J Nucl Med* **39**: 277P.

Carson RE (1986). Parameter estimation in positron emission tomography. In: Phelps ME, Mazziotta JC, Schelbert HR (eds). *Positron Emission Tomography and Autoradiography: Principles and Applications for the Brain and Heart*. Raven Press: New York. pp 347–390.

Charalambous A, Marciniak G, Shiue CY, Dewey SL, Schlyer DJ, Wolf AP *et al* (1991). PET studies in the primate brain and biodistribution in mice using (−)-5′-18F-delta 8-THC. *Pharmacol Biochem Behav* **40**: 503–507.

Cheng Y, Prusoff WH (1973). Relationship between the inhibition constant (K1) and the concentration of inhibitor which causes 50 per cent inhibition (I50) of an enzymatic reaction. *Biochem Pharmacol* **22**: 3099–3108.

Cosenza M, Gifford AN, Gatley SJ, Pyatt B, Liu Q, Makriyannis A *et al* (2000). Locomotor activity and occupancy of brain cannabinoid CB$_1$ receptors by the antagonist/inverse agonist AM281. *Synapse* **38**: 477–482.

DeLapp NW, McKinzie JH, Sawyer BD, Vandergriff A, Falcone J, McClure D *et al* (1999). Determination of [$^{35}$S]guanosine-5′-O-(3-thio)triphosphate binding mediated by cholinergic muscarinic receptors in membranes from Chinese hamster ovary cells and rat striatum using an anti-G protein scintillation proximity assay. *J Pharmacol Exp Ther* **289**: 946–955.

Dewar KM, Montreuil B, Grondin L, Reader TA (1989). Dopamine D$_2$ receptors labeled with [$^3$H]raclopride in rat and rabbit brains. Equilibrium binding, kinetics, distribution and selectivity. *J Pharmacol Exp Ther* **250**: 696–706.

Gandelman MS, Baldwin RM, Zoghbi SS, Zea-Ponce Y, Innis RB (1994). Evaluation of ultrafiltration for the free fraction determination of single photon emission computed tomography (SPECT) tracers: $\beta$-CIT, IBF, and iomazenil. *J Pharm Sci* **83**: 1014–1019.

Gatley SJ, Gifford AN, Volkow ND, Lan R, Makriyannis A (1996). $^{123}$I-labeled AM251: a radioiodinated ligand which binds *in vivo* to mouse brain cannabinoid CB$_1$ receptors. *Eur J Pharmacol* **307**: 331–338.

Gelfand EV, Cannon CP (2006). Rimonabant: a selective blocker of the cannabinoid CB$_1$ receptors for the management of obesity, smoking cessation and cardiometabolic risk factors. *Expert Opin Investig Drugs* **15**: 307–315.

Gifford AN, Makriyannis A, Volkow ND, Gatley SJ (2002). *In vivo* imaging of the brain cannabinoid receptor. *Chem Phys Lipids* **121**: 65–72.

Glass M, Dragunow M, Faull RL (1997). Cannabinoid receptors in the human brain: a detailed anatomical and quantitative autoradiographic study in the fetal, neonatal and adult human brain. *Neuroscience* **77**: 299–318.

Hawkins RA, Phelps ME, Huang S-C (1986). Effects of temporal sampling, glucose metabolic rates, and disruptions of the blood-brain barrier on the FDG model with and without a vascular compartment: studies in human brain tumors with PET. *J Cereb Blood Flow Metab* **6**: 170–183.

Herkenham M, Lynn AB, Little MD, Johnson MR, Melvin LS, de Costa BR *et al* (1990). Cannabinoid receptor localization in brain. *Proc Natl Acad Sci USA* **87**: 1932–1936.

Hirst RA, Almond SL, Lambert DG (1996). Characterisation of the rat cerebella CB$_1$ receptor using SR141716A, a central cannabinoid receptor antagonist. *Neurosci Lett* **220**: 101–104.

Horti AG, Fan H, Kuwabara H, Hilton J, Ravert HT, Holt DP *et al* (2006). $^{11}$C-JHU75528: a radiotracer for PET Imaging of CB$_1$ cannabinoid receptors. *J Nucl Med* **47**: 1689–1696.

Howlett AC, Barth F, Bonner TI, Cabral G, Casellas P, Devane WA *et al* (2002). International union of pharmacology. XXVII. Classification of cannabinoid receptors. *Pharmacol Rev* **54**: 161–202.

Katoch-Rouse R, Pavlova OA, Caulder T, Hoffman AF, Mukhin AG, Horti AG (2003). Synthesis, structure-activity relationship, and evaluation of SR141716 analogues: development of central cannabinoid receptor ligands with lower lipophilicity. *J Med Chem* **46**: 642–645.

Khawaja X, Evans N, Reilly Y, Ennis C, Minchin MC (1995). Characterisation of the binding of [$^3$H]WAY-100635, a novel 5-hydroxytryptamine1A receptor antagonist, to rat brain. *J Neurochem* **64**: 2716–2726.

Kirkham TC, Tucci SA (2006). Endocannabinoids in appetite control and the treatment of obesity. *CNS Neurol Disord Drug Targets* **5**: 272–292.

Laruelle M, Baldwin RM, Rattner Z, Al-Tikriti MS, Zea-Ponce Y, Zoghbi SS *et al* (1994). SPECT quantification of [$^{123}$I]iomazenil binding to benzodiazepine receptors in nonhuman primates. I. Kinetic modeling of single bolus experiments. *J Cereb Blood Flow Metab* **14**: 439–452.

Le Foll B, Goldberg SR (2005). Cannabinoid CB1 receptor antagonists as promising new medications for drug dependence. *J Pharmacol Exp Ther* **312**: 875–883.

Q3

Q2

Mathews WB, Scheffel U, Finley P, Ravert HT, Frank RA, Rinaldi-Carmona M *et al* (2000). Biodistribution of [$^{18}$F] SR144385 and [$^{18}$F] SR147963: selective radioligands for positron emission tomographic studies of brain cannabinoid receptors. *Nucl Med Biol* **27**: 757–762.

Mathews WB, Scheffel U, Rauseo PA, Ravert HT, Frank RA, Ellames GJ *et al* (2002). Carbon-11 labeled radioligands for imaging brain cannabinoid receptors. *Nucl Med Biol* **29**: 671–677.

Nyberg S, Chou YH, Halldin C (2002). Saturation of striatal D$_2$ dopamine receptors by clozapine. *Int J Neuropsychopharmacol* **5**: 11–16.

Pfister JR, Makra F, Muehldorf AV, Wu H, Nelson JT, Cheung P *et al* (1995). Methanodibenzosuberylpiperazines as potent multidrug resistance reversal agents. *Bioorg Med Chem Lett* **5**: 2473–2476.

Roe M, Folkes A, Ashworth P, Brumwell J, Chima L, Hunjan S *et al* (1999). Reversal of P-glycoprotein mediated multidrug resistance by novel anthranilamide derivatives. *Bioorg Med Chem Lett* **9**: 595–600.

Sadeque AJ, Wandel C, He H, Shah S, Wood AJ (2000). Increased drug delivery to the brain by P-glycoprotein inhibition. *Clin Pharmacol Ther* **68**: 231–237.

Schinkel AH, Wagenaar E, Mol CA, van Deemter L (1996). P-glycoprotein in the blood-brain barrier of mice influences the brain penetration and pharmacological activity of many drugs. *J Clin Invest* **97**: 2517–2524.

Simoneau II, Hamza MS, Mata HP, Siegel EM, Vanderah TW, Porreca F *et al* (2001). The cannabinoid agonist WIN55,212-2 suppresses opioid-induced emesis in ferrets. *Anesthesiology* **94**: 882–887.

Tamagan G, Lu X-J, Gao Y, Amici LA, Baldwin RM, Innis RB (1999). Potential SPECT radioligand for cannabinoid receptor. *J Label Compd Radiopharm* **42**: S191–S193.

Walker JM, Hohmann AG, Martin WJ, Strangman NM, Huang SM, Tsou K (1999). The neurobiology of cannabinoid analgesia. *Life Sci* **65**: 665–673.

Yasuno F, Hasnine AH, Suhara T, Ichimiya T, Sudo Y, Inoue M *et al* (2002). Template-based method for multiple volumes of interest of human brain PET images. *Neuroimage* **16**: 577–586.

Yasuno F, Zoghbi SS, JA M, Ichise M, Brown AK, Gladding RL *et al* (2006). Quantification of serotonin 5-HT$_{1A}$ receptors in monkey brain with [$^{11}$C](*R*)-()-RWAY. *Synapse* **60**: 510–520.

Zoghbi SS, Baldwin RM, Seibyl JS, Charney DS, Innis RB (1993). A radiometric technique for determining apparent pKa of receptor-binding ligands. *J Label Compd Radiopharm* **40S**: 136–138.

Zoghbi SS, Shetty HU, Ichise M, Fujita M, Imaizumi M, Liow J-S *et al* (2005). PET imaging of the dopamine transporter with [$^{18}$F]FECNT: a polar radiolabeled metabolite confounds brain radioligand measurements. *J Nucl Med* **47**: 520–527.

Q4